Ca^{2+} sensors of L-type Ca^{2+} channel

Christoph Romanin[a], Roland Gamsjaeger[a], Heike Kahr[a], Daniela Schaufler[a], Olga Carlson[b], Darrell R. Abernethy[b], Nikolai M. Soldatov[b,*]

[a] *Institute for Biophysics, University of Linz, Altenbergerstrasse 69, A-4040 Linz, Austria*
[b] *National Institute on Aging, NIH, 5600 Nathan Shock Drive, Baltimore, MD 21224-6825, USA*

Received 13 October 2000; accepted 13 November 2000

First published online 8 December 2000

Edited by Maurice Montal

Abstract **Ca^{2+}-induced inactivation of L-type Ca^{2+} is differentially mediated by two C-terminal motifs of the α_{1C} subunit, L (1572–1587) and K (1599–1651) implicated for calmodulin binding. We found that motif L is composed of a highly selective Ca^{2+} sensor and an adjacent Ca^{2+}-independent tethering site for calmodulin. The Ca^{2+} sensor contributes to higher Ca^{2+} sensitivity of the motif L complex with calmodulin. Since only combined mutation of both sites removes Ca^{2+}-dependent current decay, the two-site modulation by Ca^{2+} and calmodulin may underlie Ca^{2+}-induced inactivation of the channel.**

Key words: Heart; Calcium channel; Calmodulin; Ca^{2+} sensor; Inactivation

1. Introduction

The voltage-gated L-type Ca^{2+} channel is an oligomeric complex composed of the pore-forming α_{1C} and auxiliary β and α2-SS-δ subunits [1]. Similar to the channel initially described in *Paramecium* [2], the α_{1C} channel is inhibited by Ca^{2+} but not by Ba^{2+} ions on the cytoplasmic side of the pore [3–6]. This Ca^{2+}-induced inactivation serves as an important feedback mechanism against Ca^{2+} overloading of the cell.

The α_{1C} subunit is built of over 50 exons [7]. Alternative splicing of exons 40–42 causing substitution of 80 amino acids (1572–1651) in the C-terminal tail of the conventional $\alpha_{1C,77}$ channel [8] for 81 different amino acids deprives the channel of Ca^{2+}-induced inactivation [9]. Within these 80 amino acids there are two sequences, L (1572–1587) and K (1599–1651), independently critical for Ca^{2+}-induced inactivation [10]. A calmodulin (CaM)[1] binding IQ-like region was proposed within the sequence K [11]. The role of CaM as important mediator of Ca^{2+}-induced inactivation of the channel and its binding in the presence of Ca^{2+} to the IQ-like peptide were later confirmed [12–14]. However, the mechanism of Ca^{2+}-induced inactivation remains unclear in part because it is not understood (i) whether motif L is involved in CaM-mediated regulation of inactivation, (ii) the location or role of CaM in the resting state of the channel when the intracellular free Ca^{2+} concentration ($[Ca^{2+}]_i$) is critically low for the occupancy of the IQ region, and (iii) how the rise in $[Ca^{2+}]_i$ is transduced by CaM into inactivation of the channel.

In this study we found that motif L serves both as a Ca^{2+} sensor and CaM-binding site at low resting $[Ca^{2+}]$. Increase in $[Ca^{2+}]$ causes conformational rearrangement in the sensor which is apparently transduced to higher affinity of CaM interaction with motif L. We conclude that Ca^{2+}-dependent transition in the Ca^{2+} sensor of motif L may underlie CaM-mediated Ca^{2+}-induced inactivation of the channel.

2. Materials and methods

2.1. DNA constructs

Kozak sequence (5′-CCGCCA-3′) was incorporated at *Hin*dIII/*Nco*I sites of pHLCC77 [8] using the mixture of phosphorylated oligonucleotides 5′-AGCTTGGATCCGCCAC-3′ and 5′-CATGGTGGCGGATCCA-3′, and with the full coding sequence it was subcloned into pcDNA3 vector (Invitrogen). Mutated Ca^{2+} channel plasmid 77LpcDNA3 was prepared by ligating the 3.9-kb *Bam*HI(blunt)/*Ppu*MI fragment of pHLCC77L [10] with *Ppu*MI/*Not*I(blunt) fragment of 77pcDNA3. CaM_{WT}pcDNA3 and CaM_{Q}pcDNA3 were prepared by ligating the *Sal*I(blunt)/*Bgl*II fragments of CaM_{WT}-pBF and CaM_{Q}-pBF [15], respectively, at *Hin*dIII(blunt)/*Bam*HI sites of pcDNA3. α_{1Ca}, β_{2A} and $\alpha_2\delta$ in pcDNA3 were gifts of F. Hofmann [16].

2.2. Cell transfection and electrophysiological recording

30–50% confluent tsA201 cells were transfected with 2.5 μg of total cDNA (molar ratio of α_{1C}:β_{2A}:$\alpha_2\delta$:CaM:EGFP:CD8 = 1:1.6:1.4:4:2.5:0.7) using SuperFect (Qiagen). Transfection efficiency was estimated by EGFP fluorescence to be ≈20–60%. Co-expression of CD8 receptor was used to visually identify expressing cells for electrophysiological experiments by binding of anti-CD8 antibody-coated magnetic beads (Dynal). The whole-cell patch clamp bath solution contained (mM): 125 *N*-methylglucamine, 1 $MgCl_2$, 10 D-glucose, 10 HEPES, 5 CsCl, 20 $BaCl_2$ or $CaCl_2$. The pipet solution contained (mM): 60 CsCl, 1 $CaCl_2$, 11 EGTA, 10 HEPES, 50 aspartic acid, 5 MgATP, pH 7.4 (CsOH). Maximum activation of the $\alpha_{1C,77}$ and $\alpha_{1C,77L}$ channel currents was obtained by depolarizations to 20/20 mV and 20/30 mV with Ba^{2+}/Ca^{2+} as charge carrier, respectively.

2.3. Glutathione S-transferase (GST) pulldown

GST-$\alpha_{1C(1414-1649)}$ fusion protein was expressed using the *Eco*RV (4541)/*Fsp*I (5247) fragment of α_{1Ca} subcloned into pGEX vector (Pharmacia). GST-$\alpha_{1C(1414-1649)}$ was immobilized on glutathione–Sepharose, incubated with CaM for 2 h in 150 mM NaCl, 50 mM Tris–HCl, pH 8.0 containing 100 μM Ca^{2+} or 2 mM EGTA, and washed with the same buffer containing 0.05% Tween-20. Bound proteins were separated by SDS–polyacrylamide gel electrophoresis (PAGE) (12%) and identified by Western blot analysis with anti-CaM (Upstate Biotechnology) or anti-GST antibodies (Pharmacia).

2.4. Peptide–CaM binding PAGE shift assay

300 pmol of hog brain CaM (Pharmacia) was incubated for 30 min

*Corresponding author. Fax: (1)-410-558 8318.
E-mail: soldatov@grc.nia.nih.gov

Abbreviations: CaM, calmodulin; GST, glutathione *S*-transferase; PAGE, polyacrylamide gel electrophoresis

0014-5793/00/$20.00
PII: S0014-5793(00)02361-9

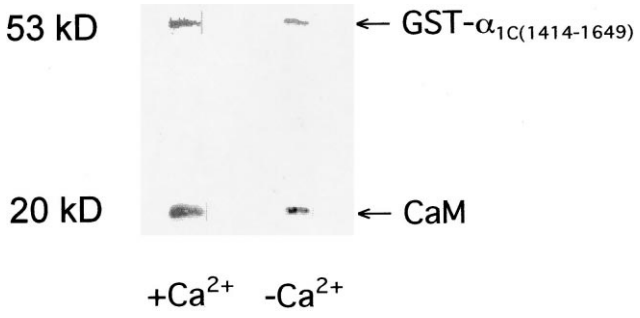

Fig. 1. Ca^{2+}-dependent and Ca^{2+}-independent binding of CaM to the α_{1C} C-terminal tail. Shown is the GST pulldown assay of CaM binding to GST-$\alpha_{1C(1414-1649)}$ fusion protein in 100 μM [Ca^{2+}] (left) or 2 mM EGTA (right). No binding of CaM to GST was detected under these conditions. Molecular weights (left) and positions (right, marked by arrows) of CaM and GST-$\alpha_{1C(1414-1649)}$ are indicated.

at 21°C with various molar excess of peptides L or K (Genemed Synthesis, Inc.) in incubation buffer (150 mM NaCl, 2 mM EGTA, 5 mM HEPES, pH 7.3) containing 50 nM ('low Ca^{2+}' buffer) or 5 μM [Ca^{2+}] ('high Ca^{2+}' buffer). Electrophoresis was carried out in 12% polyacrylamide gels in the same buffers under non-denaturing conditions. Gels were stained by Coomassie blue.

2.5. Fluorescence spectra

Fluorescence measurements were carried out on a luminescence spectrometer LS50B (Perkin Elmer Instruments). All spectra were corrected for background fluorescence.

3. Results

3.1. The C-terminal tail of the α_{1C} Ca^{2+} channel binds CaM in the presence and in the absence of Ca^{2+} ions

A GST pulldown assay using a fusion protein of GST and the C-terminal part of α_{1C} have shown (Fig. 1) that the α_{1C}

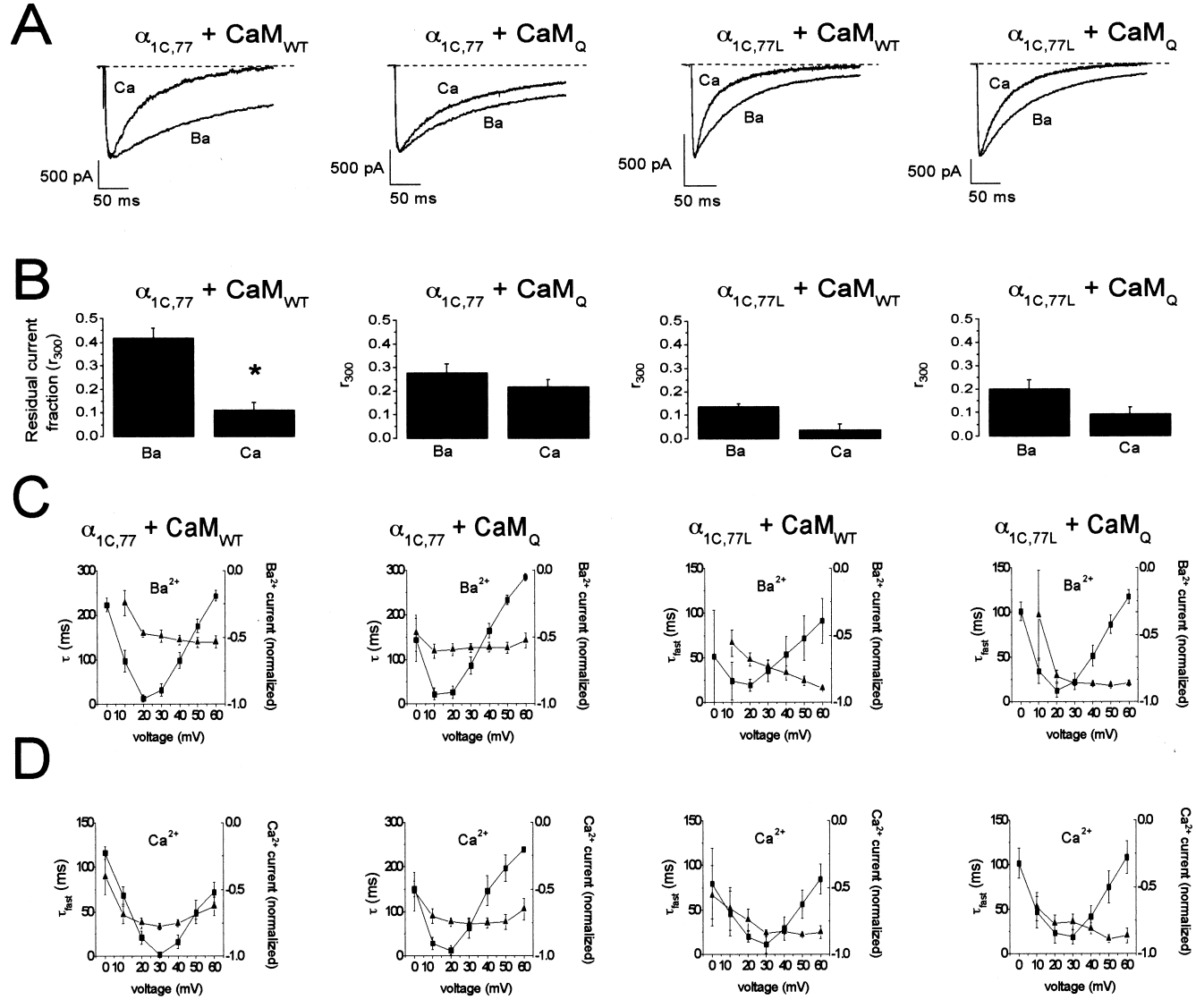

Fig. 2. Mutation of the $\alpha_{1C,77}$ channel to $\alpha_{1C,77L}$ impaired effects of Ca^{2+} and CaM on inactivation. A: Normalized Ba^{2+} and Ca^{2+} currents through $\alpha_{1C,77}$ and $\alpha_{1C,77L}$ co-expressed with auxiliary subunits and either CaM_{WT} or CaM_Q. Maximum currents were elicited by 300 ms depolarizations from a holding potential of −80 mV. B: Respective fractions of the currents (mean ± S.E.M. of three or four experiments) remaining at the end of 300 ms depolarization (r_{300}). Differences between r_{300} values of Ba^{2+} and Ca^{2+} currents are significant (asterisk, $P < 0.01$) only with $\alpha_{1C,77}$ channels co-expressed with CaM_{WT}. C: Voltage-dependence of Ba^{2+}/Ca^{2+} inward currents (■) and their inactivation time constants (▲) for $\alpha_{1C,77}$ and $\alpha_{1C,77L}$ channels co-expressed with CaM_{WT} or CaM_Q. A monotonic decrease in inactivation time constants with increasing voltage reflects voltage-dependent inactivation. An U-shape voltage-dependence of τ, observed only in Ca^{2+}-containing solution with $\alpha_{1C,77}$ channel+CaM_{WT}, is due to Ca^{2+}-dependent inactivation. Inactivation of Ba^{2+} currents through $\alpha_{1C,77}$ channels was better fit by one time constant, all other current traces were fit by two time constants with the fast ones shown. (mean ± S.E.M. of five or six experiments).

segment (1414–1649) incorporating motifs L and K, binds CaM not only in the presence of Ca^{2+} [13] but in some preparations also in Ca^{2+}-free buffer (2 mM EGTA). Repeated experiments on GST-$\alpha_{1C(1414-1649)}$ suggest critical importance for the expressed protein of either correct folding or prior removal of bound Ca^{2+} to reveal CaM binding in Ca^{2+}-free media. This finding suggests the presence of an additional Ca^{2+}-independent tethering site for CaM in the C-terminal tail of the α_{1C} channel besides the Ca^{2+}-dependent CaM-binding IQ region.

3.2. CaM is essential for Ca^{2+}-induced inactivation mediated by motif L (1572–1587) of the C-terminal tail of α_{1C}

To establish whether motif L plays a role in CaM-modulation of Ca^{2+}-induced inactivation, we compared the $\alpha_{1C,77}$ channel and its motif L-mutated isoform $\alpha_{1C,77L}$ [10] transiently co-expressed in tsA201 cells with wild-type CaM_{WT} or its inactive derivative CaM_Q [15] in which four Ca^{2+}-binding EF-hand motifs were mutated. Whole-cell recordings of Ca^{2+} and Ba^{2+} currents (Fig. 2) showed characteristic acceleration of inactivation of the $\alpha_{1C,77}$ channel by CaM_{WT} but not CaM_Q, when Ca^{2+} was substituted for Ba^{2+} as charge carrier. Under the same conditions, the $\alpha_{1C,77L}$ channel containing an intact CaM-binding IQ region exhibited only a small Ca^{2+}-dependent increase in inactivation which was rather unrelated to the type of CaM co-expressed. Analysis of residual currents (r_{300}, Fig. 2B) and voltage-dependence of inactivation time constants (τ, Fig. 2C) showed characteristics typical of Ca^{2+}-induced inactivation for the $\alpha_{1C,77}$ channel co-expressed with CaM_{WT} but not CaM_Q. In contrast, neither a significant increase in r_{300} (Fig. 2B) with Ca^{2+} as charge carrier nor the classical U-shape of voltage-dependence of inactivation time constants (Fig. 2D) was found for the $\alpha_{1C,77L}$ channel co-expressed with either CaM_{WT} or CaM_Q. These data confirm our earlier conclusion [10] of independent involvement of motifs L and K in Ca^{2+}-induced inactivation and suggest that these motifs may be differentially modulated by CaM.

3.3. CaM binds to the C-terminal region of motif L of the α_{1C} channel

To verify directly whether motif L interacts with CaM, we used synthetic peptides (Fig. 3A) which have been designed based on our segmental mutation analysis of Ca^{2+}-induced inactivation of the α_{1C} channel [10]. LA peptide represents full amino acid sequence of the motif L, while shorter peptides LM1 and LM3 comprise N- and C-terminal parts of motif L (Fig. 3A) and, respectively, incorporate M1 and M3 segments critical for Ca^{2+}-induced inactivation [10]. For comparison, we used peptide L^{86} (RETELSSQVQYQAKEA), which contains amino acids replacing motif L in $\alpha_{1C,77L}$ [10]. Fig. 3B shows results of the PAGE shift assay under non-denaturing conditions of CaM preincubated with peptides in media containing physiologically relevant 'resting' (50 nM) and 'active' (5 μM) [Ca^{2+}]. In low Ca^{2+} medium (50 nM [Ca^{2+}]), both peptides LA and LM3 bind to CaM thus increasing its size which caused a decrease in electrophoretic mobility of the complex on a non-denaturing PAGE (Fig. 3B, left). Since both LA and LM3 carry high positive charge at neutral pH (p*I* 10.2 and 9.9, respectively), they have tendency to move to cathode in upward direction out of the gel. Efficiency of CaM binding therefore can be estimated by a reduction of the CaM band with the increase in peptide/CaM molar ratio. Peptide LM1, however, carries net negative charge at neutral pH (p*I* = 4.9) and its position on the gel (marked by an arrow) is clearly seen. However, CaM band remains equally stained by Coomassie blue even at very high LM1/CaM ratios (Fig. 3B, lower left). In high Ca^{2+} medium, both peptides LA and LM3 retain their CaM-binding property. Notable CaM gel

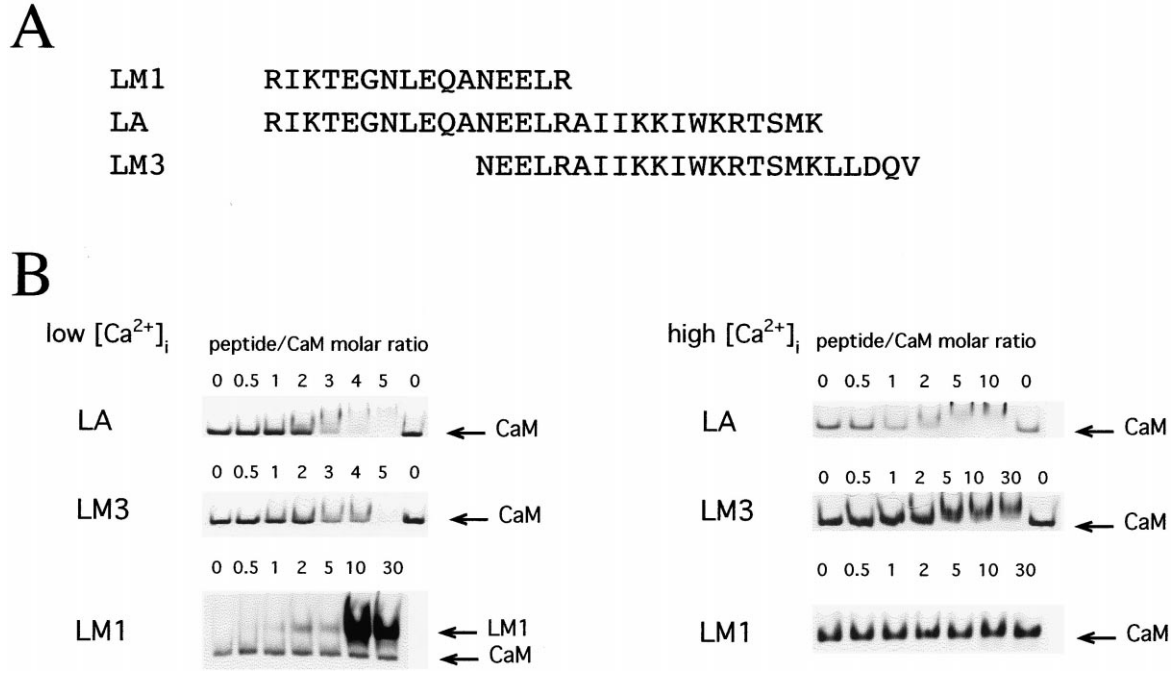

Fig. 3. CaM interacts with the C-terminal half of the motif L of the α_{1C} Ca^{2+} channel tail. A: Amino acid sequences of the motif L-derived peptides. M1 and M3 denote identified earlier [10] segments critical for Ca^{2+}-induced inactivation of the channel. B: PAGE-shift assay demonstrating Ca^{2+}-dependence of CaM interaction with peptides LA and LM3 in low [Ca^{2+}] (left) and high [Ca^{2+}] (right) media at different peptide:CaM ratios. Arrows show unbound CaM and LM1.

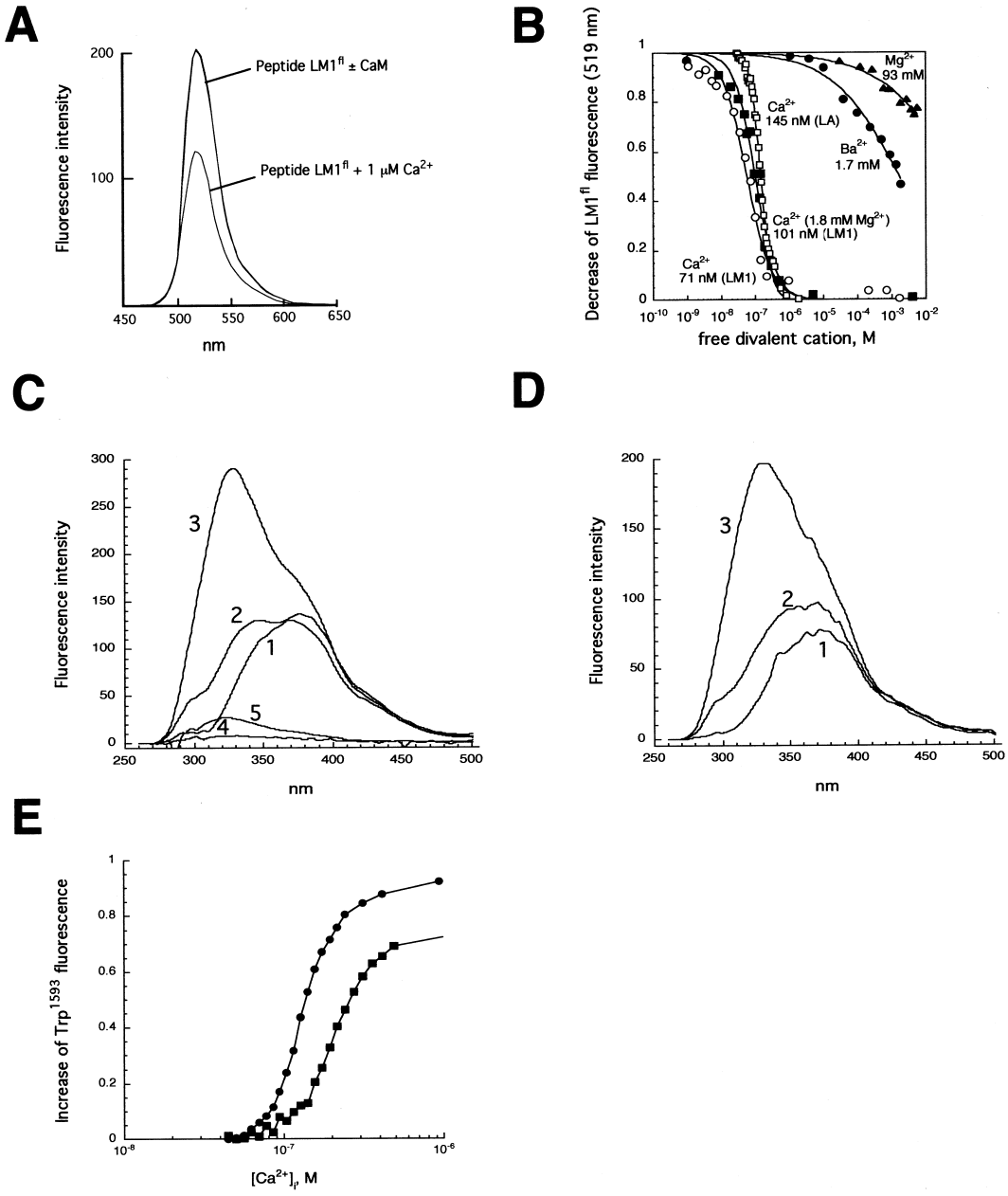

Fig. 4. Effect of divalent cations on motif L-derived peptides. A: Emission fluorescence spectra of peptide $LM1^{fl}$ (250 nM in 2 mM EGTA, 100 mM NaCl and 10 mM HEPES, pH 7.38; $\lambda_{ex} = 494$ nm) demonstrating lack of the effect of 250 nM CaM after a 30 min incubation, and $\approx 50\%$ decrease of the peak fluorescence by 1 μM $[Ca^{2+}]$. B: Dependence of normalized peak fluorescence of peptide $LM1^{fl}$ at 519 nm on $[Ca^{2+}]$ (○), $[Ba^{2+}]$ (●), $[Mg^{2+}]$ (▲) or $[Ca^{2+}]$ in the presence of 1.8 mM $[Mg^{2+}]$ (■) (23°C). For comparison, dependence of normalized peak fluorescence of peptide LA^{fl} at 519 nm on $[Ca^{2+}]$ is shown (□). Curves were fitted by equation $y = 1-(1/(1+(K_d/x)^n))$, where n: Hill coefficient. $[Cation^{2+}]$ was calculated using on-line program Webmaxc2 (www.stanford.edu/~cpatton). C: Fluorescence spectra of Trp^{1593} in LA in low Ca^{2+} medium (1), in the presence of 14 μM CaM (2) and in the presence of 14 μM CaM+1 μM $[Ca^{2+}]$ (3). Shown are also spectra of CaM (2 μM) in low Ca^{2+} medium (4) and in 1 μM $[Ca^{2+}]$ (5); $\lambda_{ex} = 295$ nm. D: Fluorescence spectra of Trp^{1593} in LM3 in low Ca^{2+} medium (1), in the presence of 14 μM CaM (2) and in the presence of 14 μM CaM+1 μM $[Ca^{2+}]$ (3); $\lambda_{ex} = 295$ nm. All spectra are corrected for background fluorescence. E: Dependence of normalized peak Trp^{1593} fluorescence of LA (●) and LM3 (■) on $[Ca^{2+}]$. At $[Ca^{2+}] > 1$ μM, LM3 shows significant contribution of the lower affinity binding which was not immediately apparent in LA and is not further discussed.

shifts caused by LA in 5 μM $[Ca^{2+}]_i$ (Fig. 3B, upper right) occur at lower molar ratio than in low Ca^{2+} medium (Fig. 3B, upper left) suggesting higher affinity of CaM to LA in 5 μM $[Ca^{2+}]_i$. In high Ca^{2+} medium, LM1 did not cause any visible gel shift of CaM (Fig. 3B, lower right). Under none of these conditions, did the control peptide L^{86} exhibit appreciable binding to CaM (not shown). These data are in accordance with the GST pulldown experiment (Fig. 1) and suggest that the C-terminal portion of motif L may serve as a tethering site for CaM at both resting (closed) and active (open) states of the channel when $[Ca^{2+}]_i$ rise from low (50–100 nM) to high (1–5 μM) levels.

3.4. Ca^{2+} sensor in the N-terminal region of motif L of the α_{1C} channel

Interestingly, free peptide LM1 did not enter the gel in 5 μM

[Ca^{2+}] (Fig. 3B, lower right). This could be due to an interaction with Ca^{2+}, which would change the peptide's net charge (−1 at pH 7) to positive at neutral pH. To investigate whether motif L is indeed sensitive to Ca^{2+}, we have studied the Ca^{2+}-dependence of fluorescence of the N-terminally fluorescein-labeled peptides $LM1^{fl}$ and LA^{fl} (Fig. 4). The peak fluorescence of $LM1^{fl}$ was quenched by Ca^{2+} independently of CaM (Fig. 4A) with apparent K_d of 71 ± 4 nM and a Hill coefficient of 1.3 ± 0.1 ($n = 4$) (Fig. 4B, ○). Physiological 1.8 mM [Mg^{2+}] slightly shifted the [Ca^{2+}]-dependence to $K_d = 101 \pm 2$ nM ($n = 3$; Fig. 4B, ■), i.e. to the range typical for the resting $[Ca^{2+}]_i$. Much weaker specificity for Ba^{2+} ($K_d \approx 1{,}7$ mM) or Mg^{2+} ($K_d \approx 93$ mM) determined from the peptide $LM1^{fl}$ titration at 519 nm (Fig. 4B) conforms to the lack of these ions effect on Ca^{2+} channel inactivation. Essentially similar data were obtained for LA^{fl}, which fluorescence was quenched by Ca^{2+} independently of CaM with apparent K_d of 147 ± 3 nM (Fig. 4B, □). These data suggest that motif LM1 is a new, highly selective Ca^{2+} sensor of the channel.

3.5. Possible role of Ca^{2+} sensor for CaM binding and Ca^{2+}-induced conformational change of motif L of the α_{1C} channel

Presence of a single Trp^{1593} residue in the C-terminal CaM-binding region of peptide LA allows to monitor conformational rearrangements in the vicinity of this amino acid that would change its fluorescence properties. Maximum of fluorescence of Trp^{1593} in peptide LA was observed at ≈380 nm (Fig. 4C, curve 1), which suggests exposure of this chromophore to hydrogen bonding groups or water. Since peptide LM3 lacking the 11 amino acid N-terminal sequence of LA (Fig. 3A) has the same maximum as peptide LA (Fig. 4D, curve 1), Ca^{2+} sensor does not appear to contribute to the spectral properties of the Trp^{1593}. Fluorescence spectra of neither LA nor LM3 were appreciably changed in the presence of 2 mM [Ca^{2+}] thus indicating an apparent lack of a conformational link between the N-terminal Ca^{2+} sensor and C-terminal CaM-binding region of LA.

Titration of LA with CaM, which does not contain Trp residues, in low [Ca^{2+}] medium caused blue shift of the spectral maximum of Trp^{1593} that may reflect its shielding due to the binding of CaM. Indeed, changes in the peak fluorescence of Trp^{1593} induced in LA (Fig. 4C, curve 2) and LM3 (Fig. 4D, curve 2) by CaM in 50 nM [Ca^{2+}] occur with very similar apparent K_d of 3.6 ± 0.2 and 3.0 ± 0.3 μM, respectively. To find whether the presence of Ca^{2+} sensor in the N-terminal part of LA does affect Ca^{2+} sensitivity of the complex of motif L with CaM, we monitored changes in Trp^{1593} fluorescence in LA and LM3 in the presence of CaM upon titration with Ca^{2+} (Fig. 4C,D, curves 3). In both peptides, Ca^{2+} induced increase and shift of the maximum of Trp^{1593} fluorescence to 328 nm, which occurred with apparent K_d of 145 ± 3 (peptide LA, ●) and 282 ± 10 nM (peptide LM3, ■) (Fig. 4E). Thus, Ca^{2+} sensor determines higher Ca^{2+} sensitivity of the interaction of CaM with motif L. This result suggests that CaM may help to extend Ca^{2+}-induced conformational changes in Ca^{2+} sensor downstream the α_{1C} channel tail to the CaM binding site, which may have direct impact on Ca^{2+}-dependent inactivation of the channel.

4. Discussion

It appears that CaM, probably only in its Ca^{2+}-bound form, is able to transduce the conformational changes caused in Ca^{2+} sensor by the permeating Ca^{2+} ions, when [Ca^{2+}] rises above the resting ≈100 nM. An immediately apparent result of this CaM-mediated transduction is a two-fold increase in the affinity of the CaM binding site of motif L monitored as a dramatic change in surroundings of Trp^{1593}. The combined effect of Ca^{2+} sensor and CaM may be of critical importance for the Ca^{2+}-induced inactivation of the α_{1C} channel. Indeed, segment-exchange mutation in either Ca^{2+} sensor or CaM-binding regions of motif L each caused only partial loss of Ca^{2+}-induced inactivation [10] indicating that neither of the two structures alone is ultimately critical for the Ca^{2+}-dependence of the current decay. Only when applied together, did these mutations produce complete loss of Ca^{2+} sensitivity and its CaM-dependence as it is shown in Fig. 2 for the $\alpha_{1C,77L}$ channel.

The combined effect of Ca^{2+} on Ca^{2+} sensor of motif L in the resting cell ($K_d \approx 100$ nM) together with a large conformational change of CaM [17–19] from the extended shape to a globular structure wrapping around the target peptide (upon binding of 3 or 4 Ca^{2+} when $[Ca^{2+}]_i$ increases above 500 nM) provides further insight into the complex nature of Ca^{2+}-dependent inactivation. Given that the L region is conserved among all dihydropyridine-sensitive Ca^{2+} channels of class C, D and S, the two-site modulation by Ca^{2+} and CaM that we propose here may be general to their Ca^{2+}-dependent regulation. The question of how the rise in $[Ca^{2+}]_i$ is transduced by CaM into inactivation of the channel may require major crystallographic and NMR studies to be elucidated. We have shown recently that mutations in the CaM-binding L or K regions leading to removal of Ca^{2+}-induced inactivation reduce single channel conductance by 15–20% [20]. These data may reflect interaction between the pore region and cytoplasmic L/K sequences of the channel. A disruption of this interaction leading to the closing of the channel may be promoted by an involvement of the recently described [21] VVTL sequence in the EF-hand region, or to other yet unidentified positions that may be closer to the pore.

Acknowledgements: We thank F. Hofmann (Munich, Germany) for gifts of α_{1Ca}, β_{2A} and $\alpha_2\delta$ in pcDNA3, and J.P. Adelman and J. Maylie (Portland, OR, USA) for kindly providing CaM_{WT}-pBF and CaM_Q-pBF plasmids. This work was supported in part by Austrian Science Foundation P12728-MOB, NB 7000, Stadt Linz and Land OÖ (C.R.) and Intramural Research Program, NIA (N.M.S.).

References

[1] Catterall, W.A. (1991) Science 253, 1499–1500.
[2] Eckert, R. and Chad, J.E. (1984) Prog. Biophys. Mol. Biol. 44, 215–267.
[3] Neely, A., Olcese, R., Wei, X.Y., Birnbaumer, L. and Stefani, E. (1994) Biophys. J. 66, 1895–1903.
[4] Zhou, J., Olcese, R., Qin, N., Noceti, F., Birnbaumer, L. and Stefani, E. (1997) Proc. Natl. Acad. Sci. USA 94, 2301–2305.
[5] Zong, X.G. and Hofmann, F. (1996) FEBS Lett. 378, 121–125.
[6] Höfer, G.F., Hohenthanner, K., Baumgartner, W., Groschner, K., Klugbauer, N., Hofmann, F. and Romanin, C. (1997) Biophys. J. 73, 1857–1865.
[7] Soldatov, N.M. (1994) Genomics 22, 77–87.
[8] Soldatov, N.M., Bouron, A. and Reuter, H. (1995) J. Biol. Chem. 270, 10540–10543.

[9] Soldatov, N.M., Zühlke, R.D., Bouron, A. and Reuter, H. (1997) J. Biol. Chem. 272, 3560–3566.
[10] Soldatov, N.M., Oz, M., O'Brien, K.A., Abernethy, D.R. and Morad, M. (1998) J. Biol. Chem. 273, 957–963.
[11] Zühlke, R.D. and Reuter, H. (1998) Proc. Natl. Acad. Sci. USA 95, 3287–3294.
[12] Zühlke, R.D., Pitt, G.S., Deisseroth, K., Tsien, R.W. and Reuter, H. (1999) Nature Lond. 399, 159–162.
[13] Peterson, B.Z., DeMaria, C.D., Adelman, J.P. and Yue, D.T. (1999) Neuron 22, 549–558.
[14] Qin, N., Olcese, R., Bransby, M., Lin, T. and Birnbaumer, L. (1999) Proc. Natl. Acad. Sci. USA 96, 2435–2438.
[15] Xia, X.-M., Fakler, B., Rivard, A., Wayman, G., Johnson-Pais, T., Keen, J.E., Ishii, T., Hirschberg, B., Bond, C.T., Lutsenko, S., Maylie, J. and Adelman, J.P. (1998) Nature Lond. 395, 503–507.
[16] Zong, X.G., Schreieck, J., Mehrke, G., Welling, A., Schuster, A., Bosse, E., Flockerzi, V. and Hofmann, F. (1995) Pflüg. Arch. 430, 340–347.
[17] Pate, P., Zhang, J.-Z. and Hamilton, S.L. (2000) Biophys. J. 78, 427A.
[18] Babu, Y.S., Sack, J.S., Greenhough, T.J., Bugg, C.E., Means, A.R. and Cook, W.J. (1985) Nature 315, 37–40.
[19] Elshorst, B., Hennig, M., Försterling, H., Diener, A., Maurer, M., Schulte, P., Schwalbe, H., Griesinger, C., Krebs, J., Schmid, H., Vorherr, T. and Carafoli, E. (1999) Biochemistry 38, 12320–12332.
[20] Kepplinger, K.J.F., Kahr, H., Förstner, G., Sonnleitner, M., Schindler, H., Schmidt, T., Groschner, K., Soldatov, N.M. and Romanin, C. (2000) FEBS Lett. 477, 161–169.
[21] Peterson, B., Lee, J., Mulle, J., Wang, Y., de Leon, M. and Yue, D. (2000) Biophys. J. 78, 1906–1920.